Can a local depletion in protosola nebular explain the low mass of Mars?

André Izidoro, Nader Haghighipour, Othon C. Winter and Masayoshi Tsuchida
São Paulo State University - Grupo de Dinâmica Orbital e Planetologia- Guaratinguetá-SP, Brazil

ABSTRACT

Models of the collision and growth of planetary embryos have been successful to produce terrestrial-class planets with sizes in the range of Venus and Earth. However, these models fail to produce a Mars analog. The body that is usually produced around the current Mars' semi-major axis through most simulations is in general too massive when compared to the mass of Mars. Only when unlike in our solar system, Jupiter and Saturn are initially considered in eccentric orbits, Mars-like objects are produced. The recently proposed Grand-Tack model tries to overcome this difficulty by allowing Jupiter and Saturn to migrated inward-then-outward. However, that scenario may not entirely agree with the models of the formation and migration of giant planets. In this paper, we present a new scenario, suggesting that a local depletion in the density of the protosolar nebula in the region of Mars can result in a non-uniform formation of embryos which will ultimately result in the formation of Mars-sized objects. We have carried out extensive numerical simulations of the formation of terrestrial planets in such a disk for different local density depletion, and for different orbital configurations of giant planets. Results of our simulations indicate that it is possible to form Mars-sized bodies along with Earth-like planets with substantial amount of water depending on the characteristics of our disk of embryos and planetesimals. We present the results of our study and discuss their implications for the formation of terrestrial planets and water delivery in our solar system.

Simulations of Terrestrial Planet Formation

According to theories of planet formation, the planetary formation can divided in stages:

(i) from dust to planetesimal;

(ii) runaway and oligarch growth scenarios from planetesimals to formation of embryos with mass ranging from Moon to Mars size;

(iii) high velocity collisions of embryos and the formation of planets or planetary cores with masses of the order of up to $10M_\oplus$ (Lissauer, 1993; Armitage, 2007).

The simulations in this paper describe the beginning of accretion late-stage of terrestrial planets formation and initially represent a transition between the stages (ii) and (iii).
We followed a distribution of mass proportional to r as $r^{-3/2}$ and the disk extends from 0.5AU to 4.0AU. The embryos' mass scale as $M \sim r^{3/2(2-\alpha)}\Delta^{3/2}$ (Kokubo & Ida, 2000, Raymond et al., 2005, 2009). The disk of embryos and planetesimals has a non-uniform distribution of mass as proposed in Jin et al. (2008). In order to represent the local depletion in mass of solar nebula we considered only a fraction of Σ_1 for the embryos and planetesimals formed in the depleted region and for the region with no depletion of mass the surface density at 1 AU (Σ_1) was $8g/cm^2$. The scale of depletion depend on the parameter β and varies from 100% to 20%, 100% of depletion means that the region has no mass β=0 and 20% of depletion means that we considered $\beta = 0.8$, $\beta\Sigma_1 = 0.8\Sigma_1 = 6.4g/cm^2$, instead of $\Sigma_1 = 8g/cm^2$.

Table: Region and scale of depletion studied

Disk	Region	Scale
A	1.1AU to 2.1 AU	100%, 75%, 50%, 20%
B	1.3AU to 2.1 AU	100%, 75%, 50%, 35% 20%
C	1.5AU to 2.5 AU	100%, 75%, 50%, 20%

$$\Sigma(r) = \begin{cases} \Sigma_1(\frac{r}{1AU})^{-3/2}, & \textit{out of depleted region} \\ \beta\Sigma_1(\frac{r}{1AU})^{-3/2}, & \textit{depleted region} \end{cases}$$

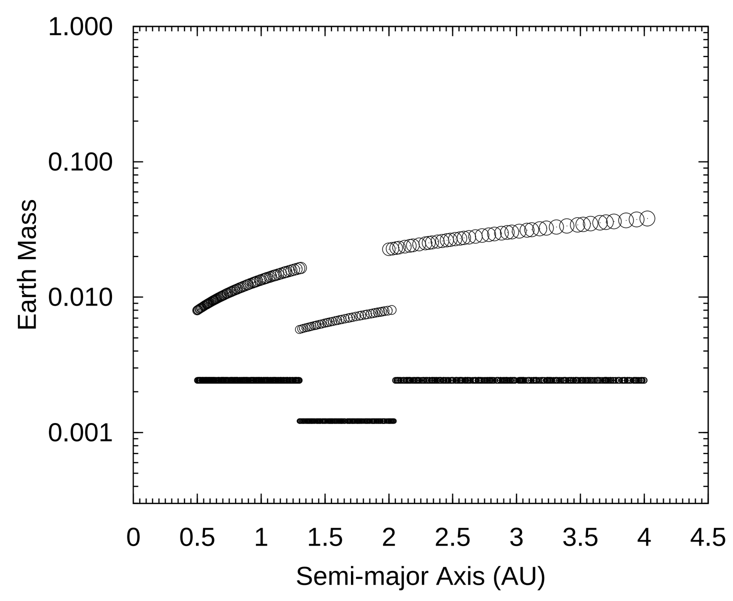

Figure: Initial distribution of 154 embryos and 973 planetesimals considering a depletion of 50% in mass from 1.3 AU to 2.0 AU. The planetesimals are shown with mass smaller than 0.0025 Earth mass.

We performed a total of 72 simulations considering two different initial orbital configuration for the giant planets. The first configuration corresponds to Jupiter and Saturn on their current orbits and in the second we considered the orbital elements of the two planets as those proposed in the Nice Model (Tsiganis et al., 2005; Gomes et al., 2005; Morbidelli et al., 2005).

Results - Dynamical Evolution

We presented the results of our simulations after 1 Gyr of integration and compared the results obtained with characteristics of the Solar System, as mass and orbital elements of planets, remnant of planetesimals in the asteroid belt region, accretion timescales for Earth and Mars and water delivery to Earth.

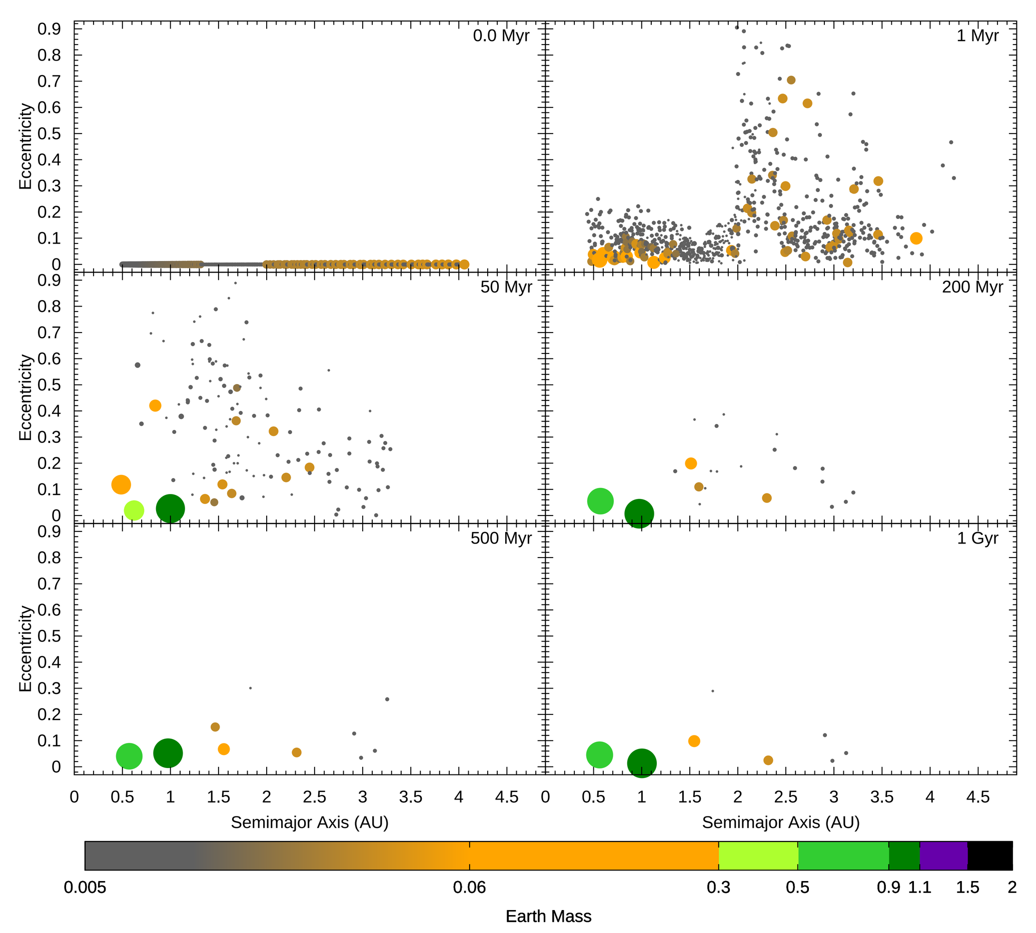

Figure: Snapshots of the dynamical evolution of a system initially with a depletion of 75% in mass from 1.3 AU to 2.1 AU, considering Jupiter and Saturn on their current positions. The size of each body corresponds to its relative physical size and is scaled as $M^{1/3}$, but it is not to scale on the x axis. The color-code used represents the mass of the body in Earth's mass.

Results

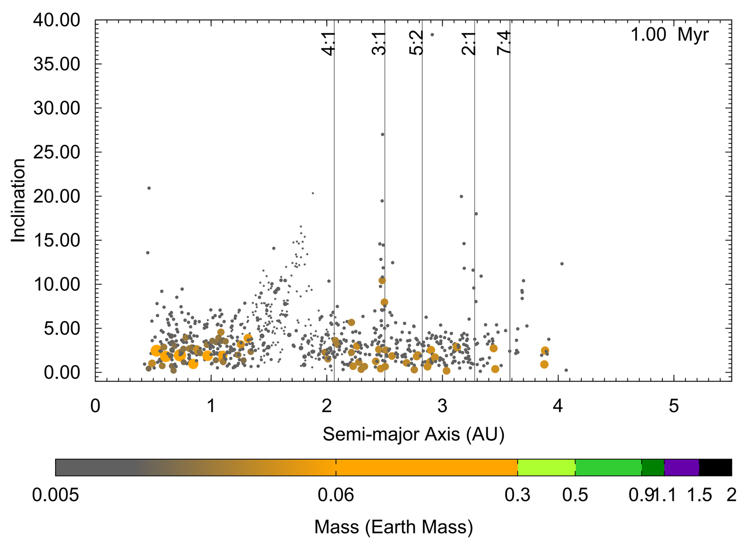

Figure: Effects of secular resonances (ν_{16}) increasing the inclination of embryos and planetesimals in depleted region at 1 Myr.

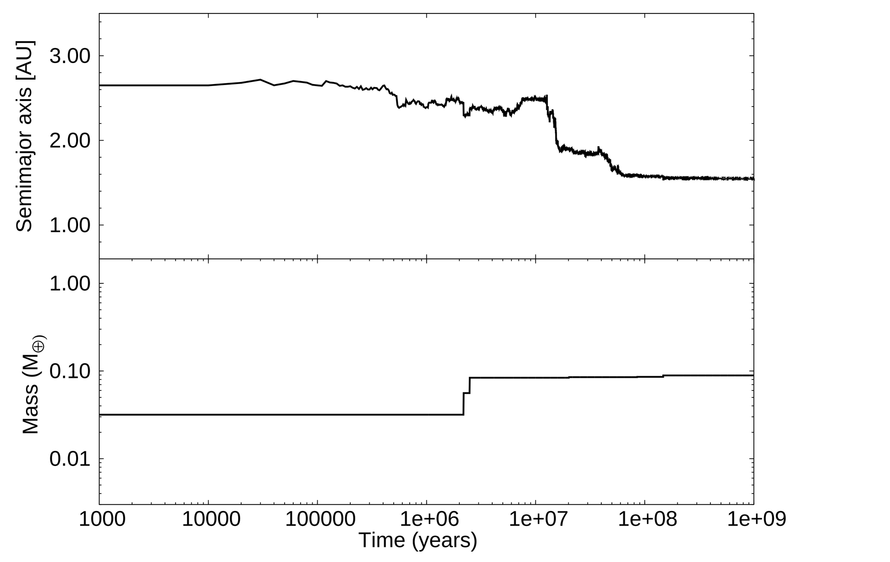

Figure: Evolution of semi-major axis and mass of a Mars analog. This is a representative behavior noted in our results. Usually Mars analogs are the scattered from outer or inner regions of disc where the depletion in mass is not considered.

Results: Disk A and Disk B

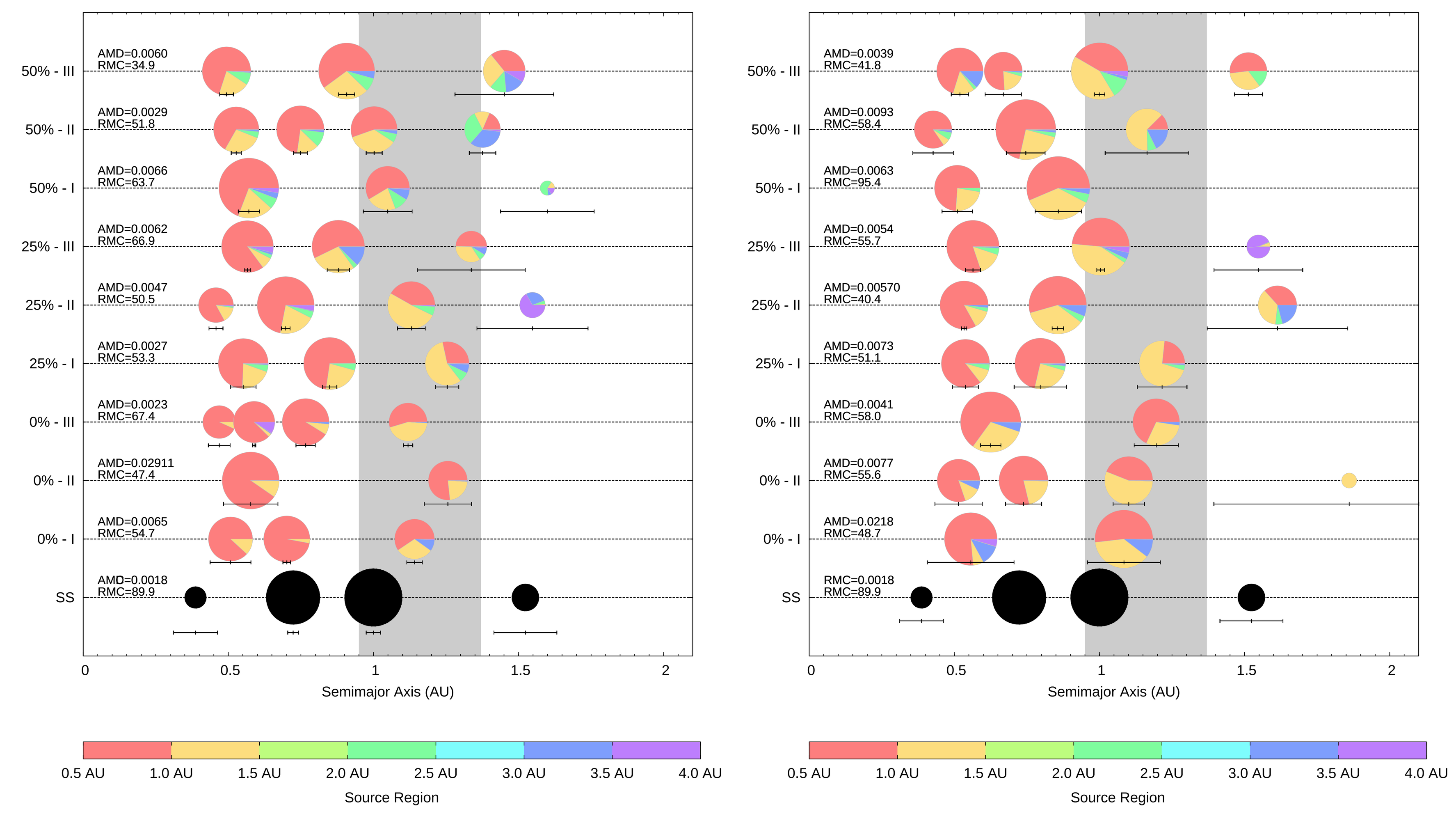

Figure: Final configuration for simulations considering a depletion in mass from 1.1 AU to 2.1 AU (left - Disk A) and 1.3 AU to 2.0 AU (right - Disk B). The results are showed for different scales of depletion after 1 billion year of integration.

The size of each body corresponds to its relative physical size scaled as $M^{1/3}$, but is not to scale on the x-axis. The color represents the relative contributions of material from different semi-major axis regions. Pie diagrams show the relative contributions of material from each region to each planet. The planet eccentricity is represented by its variation in heliocentric distance over an orbit (horizontal bars).

Conclusions

For a final analysis we defined Earth analog candidates and Mars analog candidates as planets from 0.75 AU to 1.25 AU and 1.25 AU to 2.0 AU respectively (limit cases were also considered). Following similar considerations as Raymond et al. (2009) we quantitatively evaluate how the simulations fared at reproducing seven constraints using relatively generous values: (1) $M_{Mars} < 0.3M_\oplus$, (2) $T_{form,Mars} < 10Myr$, (3) $M_{Earth} > 0.7M_\oplus$, (4) 30 Myr $< T_{form,Earth} <$ 150 Myr, (5) $WMF_{Earth} > 5\times10^{-4}$, (6) AMD$<$ 0.036 (twice the Mercury, Venus, Earth and Mars value), (7) $M_{ast} < 0.05M_\oplus$, where M_{Mars} is the mass of Mars analog candidate, $T_{form,Mars}$ is the timescale of formation of Mars analog candidate, M_{Earth} is the mass of Earth candidate, $T_{form,Earth}$ is timescale of formation of Earth candidate, WMF_{Earth} is the water mass fraction of Earth candidate, AMD is the angular momentum deficit, and M_{ast} is the mass in embryos stranded in the asteroid belt. We analyzed these constraints only for those simulations that have fared our main goal that is the formation of a small Mars, ie, to have produced at least a planet smaller than 0.3 $M_\oplus$ between 1.25 AU and 2.0 AU. When a simulation reproduce a given constraint it receives a sign "✓" or a sign "×" otherwise, for limit cases we attributed a sign "∼".

Table: Summary of results considering the region of depletion A indicating success (✓) , failure (×) or maybe (∼) in order to reproduce individual constraints

Sim.	M_{mars}	$t_{form,Mars}$	M_{Earth}	$t_{form,Earth}$	WMF_{Earth}S	AMD	M_{ast}	N_{ast}
A-25% - II	✓	✓	∼	∼	∼	×	×	1
A-25% - III	✓	×	✓	×	×	×	✓	6
A-50% - II	✓	×	×	×	×	✓	✓	4
B-25% - II	✓	×	✓	✓	×	×	×	0
B-25% - III	✓	×	✓	✓	✓	×	✓	3
B-50%- III	✓	×	✓	✓	✓	×	×	2

References

- Jin, L., Arnett, W. D., Sui, N., & Wang, X. 2008, ApJl, 674, L105
- Raymond, S. N., Quinn, T., & Lunine, J. I. 2005, ApJ, 632, 670
- Raymond, S. N., O'Brien, D. P., Morbidelli, A., & Kaib, N. A. 2009, Icarus, 203, 644
- Kokubo, E., & Ida, S. 2000, Icarus, 143, 15
- Lissauer, J. J. 1993, ARA&A, , 31, 129
- Gomes, R., Levison, H. F., Tsiganis, K., & Morbidelli, A. 2005, Nature, 435, 466
- Morbidelli, A., Levison, H. F., Tsiganis, K., & Gomes, R. 2005, Nature, 435, 462
- Tsiganis, K., Gomes, R., Morbidelli, A., & Levison, H. F. 2005, Nature, 435, 459
- Walsh, K. J., Morbidelli, A., Raymond, S. N., O'Brien, D. P., & Mandell, A. M. 2011, Nature, 475, 206

izidoro.costa@gmail.com